PHYSICAL REVIEW C

NUCLEAR PHYSICS

THIRD SERIES, VOLUME 33, NUMBER 5 MAY 1986

Validity of macroscopic models for the $^3He(\alpha,\gamma)^7Be$ electric-dipole capture reaction

Q. K. K. Liu
Bereich Physik, Hahn-Meitner-Institut, 1000 Berlin 39, Federal Republic of Germany

H. Kanada
Department of Physics, Niigata University, Niigata 950-21, Japan

Y. C. Tang
School of Physics, University of Minnesota, Minneapolis, Minnesota 55455
(Received 30 December 1985)

The cross sections for the electric-dipole radiative-capture reaction $^3He(\alpha,\gamma)^7Be$ are calculated with an approximation procedure (approximate-resonating-group-method procedure) in which the antisymmetrization of the wave function is simply represented by the adoption of an intercluster renormalized function obtained by operating on the resonating-group relative-motion function with the square root of the norm operator. The result shows that this procedure does yield values for the capture cross-section factor in excellent agreement with the resonating-group-method results. By studying the properties of the approximate-resonating-group-method wave functions, we find that, in this capture reaction, the nuclear potential is sampled at all energies and should be properly considered even at astrophysical low energies around 10 keV. In addition, based again on approximate-resonating-group-method results, we have shown that the macroscopic capture-reaction models of Iwinski *et al.* using analytical-continuation techniques and of Buck *et al.* using Gaussian-type effective local potentials are not sufficiently accurate for the computation of cross-section factors because of the fact that the details of the nuclear interaction are not well accounted for.

I. INTRODUCTION

The unresolved long-standing solar-neutrino problem has inspired in the last few years a series of detailed microscopic calculations of the radiative-capture reaction $^3He(\alpha,\gamma)^7Be$ and other electromagnetic properties of the seven-nucleon system because of the pivotal role played by the capture reaction in the production of high-energy solar neutrinos in the p-p chain solar model (see, for example, Ref. 1). These were carried out in the resonating-group-method (RGM) formalism. Simultaneously, there was also a surge of activity in the measurement of the capture reaction. On a less ambitious scale than RGM, Liu *et al.*[2] and Walliser and Fliessbach[3] used the cluster representation, but without antisymmetrization, to calculate many electromagnetic properties of the seven-nucleon system. In contrast to a calculation with the full RGM wave function, the matrix elements do not explicitly contain any exchange contribution. They have shown that their approximations to the RGM calculation of the matrix elements are, in the main, accurate in the low momentum-transfer region. The radiative capture reaction was not included in their calculations, but it seems very likely that the same excellent agreement with RGM would also have been obtained. However, this approximation requires the foreknowledge of the RGM solutions of bound and scattering problems; therefore, it is not an effective way to avoid the elaborate microscopic RGM.

It is obviously desirable to devise simple macroscopic models which include the most important features of a microscopic approach and yet have reliable predictive power. The latter aspect means that, by using at most a class of experimental data as input, we can predict with some confidence other physical information. Recent proposals by Iwinski *et al.*[4] and Buck *et al.*[5] showed promising signs of being reliable macroscopic methods to predict the radiative-capture reaction cross sections of $^3He(\alpha,\gamma)^7Be$ at energies of interest in astrophysics. These methods have important implications for future calculations of other capture reactions, e.g., the $d(\alpha,\gamma)^6Li$ reaction which is relevant to the history of the early universe[6] and which is not yet amenable to an accurate microscopic calculation.

In this work we extend the RGM-approximated (A-RGM) investigations of Liu *et al.*[2] (LKT1) and Walliser and Fliessbach[3] by evaluating the $^3He(\alpha,\gamma)^7Be$ electric-

dipole radiative capture reaction using the A-RGM wave functions. We show that the expected good agreement with RGM is realized. Although it would be misleading to compare the details of RGM calculations (which include explicit antisymmetrization) with the macroscopic calculations of Iwinski *et al.* and Buck *et al.* (which have no antisymmetrization at all), the results of the A-RGM calculations are the benchmark quantities against which macroscopic models can be tested in detail. We show that both of the macroscopic models of Iwinski *et al.* and Buck *et al.* are deficient and, with the help of the A-RGM results, point out where their failings may lie.

In Sec. II, we describe the A-RGM, and in Sec. III, the macroscopic models of Iwinski *et al.* and Buck *et al.*, and their results are compared. The differences between A-RGM and the macroscopic models are discussed in more detail in Sec. IV. In Sec. V, we present some concluding remarks.

II. THE A-RGM MODEL

Most of the discussion in this section on ^{7}Be is an exact parallel of our earlier A-RGM investigation of ^{7}Li (LKT1). The essence of the model is contained in the substitution of the RGM wave function

$$\psi_M = \mathscr{A}\bar{\psi}_M = \mathscr{A}\left\{\phi_A\phi_B\left[\frac{1}{R}f_{Jl}(R)Y^M_{Jls}\right]Z(\mathbf{R}_{\text{c.m.}})\right\} \tag{1}$$

by the A-RGM wave function

$$\hat{\psi}_M = \phi_A\phi_B\frac{1}{R}\hat{f}_{Jl}(R)Y^M_{Jls}Z(\mathbf{R}_{\text{c.m.}}) , \tag{2a}$$

where

$$\hat{f}_{Jl}(R) = n_l^{1/2}f_{Jl}(R) , \tag{2b}$$

in the evaluation of matrix elements. We denote the ground and first-excited states of ^{7}Be or the scattering state of ^{3}He + α by $\hat{\psi}_M$. The notation we use here is the same as that in Liu *et al.*[7] (LKT2). In Eq. (1), $\mathscr{A}$ is the antisymmetrization operator. The functions ϕ_A and ϕ_B describe the internal spatial structures of the α and ^{3}He clusters. They are assumed to be represented by single-Gaussian functions characterized by width parameters α_A and α_B, respectively. The RGM solution of the radial relative-motion function $f_{Jl}(R)$ can be obtained after a great deal of computation, given a many-nucleon Hamiltonian. The A-RGM relative-motion function is written as $\hat{f}_{Jl}(R)$. The central quantity in the approximation is the operator $n_l^{1/2}$. It is defined via the norm kernel $\mathscr{N}(\mathbf{R}',\mathbf{R}'')$ of Eq. (26) of LKT2. Upon a partial-wave expansion, one can write

$$\mathscr{N}(\mathbf{R}',\mathbf{R}'') = \frac{1}{R'R''}\sum_{L,\nu} n_L(R',R'')Y^\nu_L(\hat{\mathbf{R}}')Y^{\nu*}_L(\hat{\mathbf{R}}'') . \tag{3}$$

The RGM normalization of the bound state can easily be reexpressed in terms of the norm operator as

$$\langle\bar{\psi}_M \mid \psi_M\rangle = \langle f_{Jl} \mid n_l \mid f_{Jl}\rangle = 1 . \tag{4}$$

A convenient representation of the operator $n_l^{1/2}$ can be constructed from the eigenvalues and normalized eigenstates of the norm operator, i.e.,

$$n_l\chi_{Nl} = \mu_{Nl}\chi_{Nl} . \tag{5}$$

These eigenvalues and eigenstates are labeled by an ordering index N which becomes equal to the number of relative-motion oscillator quanta in the limit where the width parameters of the clusters are the same. In terms of these quantities, the operator $n_l^{1/2}$ can be written as

$$n_l^{1/2} = 1 - \sum_N (1-\sqrt{\mu_{Nl}}) \mid \chi_{Nl}\rangle\langle\chi_{Nl} \mid . \tag{6}$$

Discussions of the general properties of μ_{Nl} and χ_{Nl} have been given by Horiuchi[8] and in the special case of ^{7}Li by LKT1. It is important to remember that $n_l^{1/2}$ is a short-range operator such that the asymptotic behaviors of $f_{Jl}(R)$ and $\hat{f}_{Jl}(R)$ are identical. Part of the antisymmetrization is contained implicitly in $\hat{f}_{Jl}(R)$.

Inserting the A-RGM wave functions of Eq. (2) into the machinery of LKT2, we can easily see that the electric-dipole capture cross section is given by Eq. (45) of LKT2 without any of the exchange terms and replacing $\mid C_{J_f}\mid^2\times 7!$ by unity, while in the direct integrals all the RGM radial relative-motion functions are to be replaced by the A-RGM radial functions.

In the present A-RGM calculations, the width parameters of the ^{3}He and α clusters are 0.367 and 0.514 fm^{-2}, respectively, as in LKT2. They reproduce the rms matter

TABLE I. Calculated RGM and A-RGM results for the capture cross sections and branching ratio.

	RGM				A-RGM			
E (MeV)	$\sigma(\frac{3}{2}^-)$ (μb)	$\sigma(\frac{1}{2}^-)$ (μb)	Sum (μb)	Ratio	$\sigma(\frac{3}{2}^-)$ (μb)	$\sigma(\frac{1}{2}^-)$ (μb)	Sum (μb)	Ratio
0.10	0.000 334	0.000 139	0.000 473	0.414	0.000 333	0.000 138	0.000 471	0.415
0.15	0.004 42	0.001 83	0.006 25	0.414	0.004 41	0.001 83	0.006 24	0.415
0.20	0.0195	0.008 07	0.0276	0.414	0.0194	0.008 04	0.0274	0.415
0.50	0.464	0.194	0.658	0.417	0.461	0.193	0.654	0.418
0.75	1.052	0.444	1.496	0.422	1.045	0.442	1.487	0.423
1.70	3.047	1.334	4.381	0.438	3.013	1.322	4.335	0.439
2.06	3.722	1.641	5.363	0.441	3.673	1.623	5.296	0.442
4.00	7.044	3.115	10.159	0.442	6.851	3.041	9.892	0.444

radii of ^{3}He and α from electron-scattering experiments.[9] For the scattering waves we include both s and d waves.[10] In Table I, we show a comparison of the RGM and A-RGM results at selected energies. The very slight differences between our present RGM results and the previous ones[10] are due to a minor improvement in the numerical procedure. The excellent agreement between the RGM and A-RGM electric-dipole capture cross sections confirms our expectation from previous work.[2,3] We might have argued that, at the high energy of several MeV, where there is a rather strong overlap of the ^{3}He and α clusters, the A-RGM procedure might be too crude to describe the intricate interplay of the exchange effects. Nevertheless, we see that A-RGM errs only by approximately 2% at 4 MeV. The summed S factor $S(0)$ to the ground and excited states of ^{7}Be is obtained from extrapolating the low-energy results to zero energy with Eq. (27) of Ref. 10. We have for RGM, $S(0)=0.703$ keV b and for A-RGM, $S(0)=0.700$ keV b. The agreement between them is again excellent. The s-wave contributions to these calculations are 0.693 keV b and 0.691 keV b, respectively.

III. MACROSCOPIC MODELS

A. Analytical continuation technique (ACT)

Iwinski *et al.*[4] proposed this method which is based on the hard-core model of Tombrello and Parker.[11] In this model one assumes that at very low energies the capture takes place mainly at distances large compared with the nuclear dimension but under the Coulomb barrier. At such large separations the bound state is known to within a normalization constant to be the Whittaker function and the scattering function is known exactly in terms of Coulomb functions. Hence, there is some justification in writing the electric-dipole capture matrix element as

$$M_{HC}(E)=N_B \int_{r_0}^{\infty} W_{\rho,\lambda}(2\kappa_B R) R O_l(R,E) dR \ , \qquad (7)$$

where r_0 is chosen to be 2.8 fm, the radius of a charged hard core which yields reasonably the empirical s- and d-wave phase shifts. Here $W_{\rho,\lambda}$ denotes the Whittaker function which depends on the decay constant κ_B of the ^{7}Be bound state and the ^{3}He-α separation distance R, with ρ being the negative of the Sommerfeld parameter and $\lambda=l+\frac{1}{2}$. The function O_l represents an s or d scattering Coulomb wave with the corresponding experimental phase shift at energy E. At energies where the capture to the ground and first-excited states of ^{7}Be can be differentiated, the individual absolute cross sections would determine the two normalization constants N_B of the bound states. These are then retained for further calculations with Eq. (7) at low astrophysical energies.

The ACT of Iwinski *et al.* avoids the determination of N_B at high energy where Eq. (7) may not be valid. They used an analytical continuation of the ^{3}He+α elastic-scattering $p_{3/2}$ and $p_{1/2}$ phase shifts to determine the ground-state ($\frac{3}{2}^-$) and excited-state ($\frac{1}{2}^-$) normalization constants N_B. The degree of accuracy required of the phase shifts, they claimed, is about one degree down to an energy of about 800 keV. As a test of this procedure, they have taken the phase shifts from our RGM calculation of LKT2 as the "experimental" phase shifts and successfully reproduced the normalization constants of the two bound states of ^{7}Be given by RGM. Good agreement with the S factor from LKT2 was also reported, but unfortunately the exact figures were not published.

The assumption of Eq. (7) cannot be tested in a straightforward fashion with RGM because the latter contains exchange contributions. But Eq. (7) can be compared directly with the corresponding capture matrix element in the A-RGM calculation where the bound and scattering states are those given by Eq. (2). We shall present and discuss evidence in Sec. IV that the approximation of Eq. (7) is not accurate even in the limit of zero energy. Therefore, although the ACT has demonstrable accuracy in deriving the asymptotic normalization constant, its usefulness may be limited in the instance of the radiative capture problem.

B. Gaussian potential model

While the ACT determines directly the asymptotic normalization of the bound state without resorting to a potential, Buck *et al.*[5] set out to calculate the bound and scattering states via a macroscopic potential which they construct from a set of experimental data. The underlying assumption is the same as in A-RGM that the seven-nucleon system is well represented by a clustering picture of ^{3}He-α or t-α. They also used Gaussian functions for the description of the spatial structure of the individual clusters. In other words, their macroscopic wave functions have the same form as the A-RGM wave function in Eq. (2a). Their constructed potential would generate the bound and scattering radial relative-motion functions to be used in Eq. (2a) in place of $\hat{f}_{Jl}(R)$.

The experimental data they used are the electromagnetic properties of ^{7}Li (those of ^{7}Be are not available since it is an unstable nucleus). However, within the cluster model, this set of data, including the charge and magnetization radii, the quadrupole moment, the octupole moment, and the $B(E2)$ value for $\frac{3}{2}^-$ to $\frac{1}{2}^-$ transition, determines essentially just the mean square separation $\langle R^2\rangle$ of α and t. With the knowledge of $\langle R^2\rangle$ of ^{7}Li, the binding energies of the ground-state doublets of ^{7}Li and ^{7}Be determine uniquely the four parameters V, V_{so}, $\bar{\alpha}$, and R_C of their assumed Gaussian potential:

$$V(R)=-(V+4V_{so}\mathbf{L}\cdot\boldsymbol{\sigma})\exp(-\bar{\alpha}R^2)+V_C(R) \ , \qquad (8)$$

with

$$V_C(R)=ZZ'e^2/R \text{ for } R>R_C \ ,$$
$$=\frac{ZZ'e^2}{2R_C}[3-(R/R_C)^2] \text{ for } R<R_C \ . \qquad (9)$$

They deduced from their analysis $\langle R^2\rangle=13.5$ fm^2, $V=86.08$ MeV, $V_{so}=0.957$ MeV, $\bar{\alpha}=0.163$ fm^{-2}, and $R_C=3.248$ fm. This is the potential which generates the ground-state ($l=1$) doublet of ^{7}Be. For the scattering s wave, they found that they have to reduce the central depth to $V=67.67$ MeV in order to obtain agreement with the low-energy elastic scattering phase shifts. This is

a simulation of the strong parity-dependent effect found in RGM calculations.[12] Making use of the limiting form of the Coulomb functions at zero energy, they could calculate the S factor $S(0)$ directly without resorting to extrapolation described in Sec. II and obtained a value of $S(0)=0.47\pm0.02$ keV b. This value is indeed close to the experimentally measured values, offering tantalizing promise that this macroscopic procedure could be a reliable way to predict capture-reaction S factors, perhaps in other reactions of interest in astrophysics as well.

To establish the accuracy of the construction of Buck *et al.*, we test the procedure in the spirit of Iwinski *et al.*, i.e., we take the A-RGM results of phase shifts (identical to RGM) and $\langle R^2\rangle$ as "experimental" values which serve as input for the construction of a Gaussian potential for the bound and scattering states. For the sake of clarity, we restrict ourselves to s-wave capture. The S factor is then compared directly with the value from A-RGM. This is a more searching test because we can make use of the A-RGM results of the ^{3}He+α elastic-scattering phase shifts at energies much lower than experimentally measured so far, and $\langle R^2\rangle$ of ^{7}Be directly without appealing to ^{7}Li. Further discussion on the relation between RGM and the procedure of Buck *et al.* is given in Sec. IV.

In the procedure of Buck *et al.*, $\langle R^2\rangle$ is a crucial input in the construction of the potential. Even though $\langle R^2\rangle$ is not an observable, one can derive it from the rms matter radius calculated with the full RGM wave function because of the cluster model assumed.[2,3] Walliser and Fliessbach have demonstrated that this $\langle R^2\rangle$ from RGM is very well approximated by a direct evaluation with the A-RGM wave function. For the $\frac{3}{2}^-$ ground and $\frac{1}{2}^-$ excited states of ^{7}Be,

$$\langle R^2\rangle=\int_0^\infty \hat{f}_{Jl}(R)R^2\hat{f}_{Jl}(R)dR \ , \tag{10}$$

where $\hat{f}_{Jl}$ is the A-RGM radial function of Eq. (2), with $l=1$ and $J=\frac{3}{2}$ or $\frac{1}{2}$. The results are 14.82 and 16.38 fm^2, respectively. The value of 14.82 fm^2 is larger than 13.86 fm^2 for the $\frac{3}{2}^-$ ground state of ^{7}Li because of larger Coulomb repulsion.[3] Armed with these $\langle R^2\rangle$ values for the ground-state doublet of ^{7}Be and their energies $E(\frac{3}{2}^-)=-1.58$ MeV and $E(\frac{1}{2}^-)=-1.15$ MeV from RGM in LKT2, we determine uniquely the parameters $\bar{V}_{3/2}$, $\bar{\alpha}_{3/2}$, $\bar{V}_{1/2}$, $\bar{\alpha}_{1/2}$ in the Gaussian potentials

$$V_J(R)=-\bar{V}_J\exp(-\bar{\alpha}_J R^2) \tag{11}$$

for the $\frac{3}{2}^-$ and $\frac{1}{2}^-$ bound states. Compared with Buck *et al.*, we use different width parameters for the $\frac{3}{2}^-$ and $\frac{1}{2}^-$ potentials and represent the spin-orbit splitting by $\bar{V}_{3/2}$ and $\bar{V}_{1/2}$. The Coulomb potential is evaluated from folding the Coulomb interaction between protons into the Gaussian functions representing the ^{3}He and α clusters,[13] i.e.,

$$V_C(R)=\frac{4e^2}{R}\Phi\left[\left[\frac{12\alpha_A\alpha_B}{8\alpha_A+9\alpha_B}\right]^{1/2}R\right], \tag{12}$$

where Φ is the error function. Hence the Coulomb radius R_C is made superfluous. As it turns out, these differences are on the whole cosmetic and do not affect the main body of our discussion later. We found our parameters to be

$$\bar{V}_{3/2}=82.52 \text{ MeV}, \quad \bar{\alpha}_{3/2}=0.154 \text{ fm}^{-2}, \tag{13}$$

$$\bar{V}_{1/2}=78.28 \text{ MeV}, \quad \bar{\alpha}_{1/2}=0.149 \text{ fm}^{-2}. \tag{14}$$

We see that with these parameters our potentials are very similar to those of Buck *et al.* Following these authors we readjust the depth parameter $\bar{V}_{3/2}$ to calculate the scattering s wave. In our case we found that the depth of 65.60 MeV would reproduce the scattering length $a=28.2$ fm from RGM.[14]

With these potentials we can calculate the S factor by extrapolating from cross sections evaluated at very low energies as described in Sec. II. We obtain $S(0)=0.515$ keV b and $S_{1/2}(0)/S_{3/2}(0)=0.452$. These are to be compared with the A-RGM values of 0.691 keV b and 0.415 from Sec. II and Table I.[15]

Our value of 0.515 keV b is rather close to the value in Buck *et al.* of 0.47 keV b, perhaps confirming our conjecture that our Gaussian potentials are not greatly different from theirs. However, we constructed our potential from the A-RGM data and are aiming for the A-RGM S factor and apparently have fallen rather short. This casts doubt on our method of construction which we have adopted from Buck *et al.* In Sec. IV, we investigate the reason for the discrepancy between the results from A-RGM and the Gaussian-potential model.

IV. DISCUSSION ON THE VALIDITY OF THE MACROSCOPIC MODELS

For the investigation of the hard-core model assumed in ACT, we plot in Fig. 1 the A-RGM integrand of the s-wave capture matrix element

$$M_{\text{A-RGM}}(E)=\int_0^\infty \hat{f}_{3/2,1}(R)R\,\hat{f}_{1/2,0}(R)dR \tag{15}$$

to the $\frac{3}{2}^-$ ground state of ^{7}Be at a c.m. energy of 0.15 MeV. In Eq. (15), the bound state $\hat{f}_{3/2,1}$ is normalized to unity while the scattering state $\hat{f}_{1/2,0}$ is normalized ac-

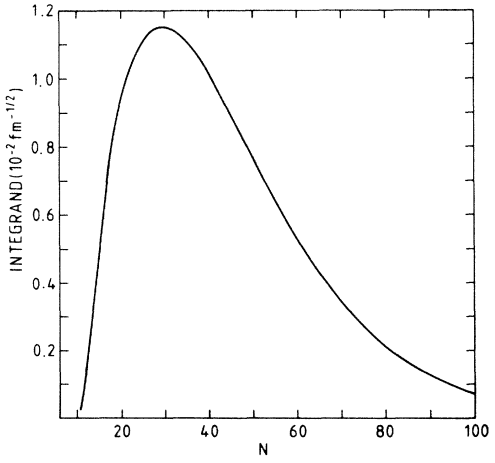

FIG. 1. The A-RGM integrand of the s-wave capture matrix element to the ^{7}Be ground state at $E=0.15$ MeV.

cording to Eq. (15) of LKT2. In Fig. 1, as in all other figures, the relative distance between ^{3}He and α is written as N, given in units of 0.24 fm. The maximum of the integrand occurs at $R=7.2$ fm ($N=30$), which is nearly twice the intercluster distance between ^{3}He and α in the ^{7}Be ground state as estimated by $\langle R^2\rangle$ in Eq. (10), confirming one of the basic assumptions of the hard-core model that at low energies capture takes place mainly under the Coulomb barrier. However, one notes that there is a significant contribution to the integral in the region $R=3.6$ to 7.2 fm ($N=15$–30). This is the region just beyond the intercluster distance of Eq. (10), where we expect the nuclear interaction to be evident still. Therefore, Eq. (7) yields a somewhat unreliable result on account of its using wave functions which are insufficiently accurate in this region, although the lower integration limit seems to be acceptable from inspection of Fig. 1.

It is particularly instructive to examine at which intercluster distances most of the capture takes place. For this purpose, we calculate the following percentage as a function of $R_{\min}$ and $R_{\max}$,

$$P=\frac{\left|\int_{R_{\min}}^{R_{\max}}\hat{f}_{3/2,1}(R)R\,\hat{f}_{1/2,0}(R)dR\right|^2}{\left|\int_0^{\infty}\hat{f}_{3/2,1}(R)R\,\hat{f}_{1/2,0}(R)dR\right|^2}\ . \tag{16}$$

In Eq. (16), the denominator is directly proportional to the A-RGM capture cross section. The lower and upper limits in the numerator are chosen such that the contributions to the capture integral of Eq. (15) from $R=0$ to $R_{\min}$ and from $R_{\max}$ to ∞ are the same. We use Eq. (16) to probe the A-RGM s-wave capture to the ^{7}Be ground state as a function of the scattering energy and plot in Fig. 2 the range $R_{\min}$ to $R_{\max}$ as a function of E for P equal to 0.5 and 0.9. It shows that the lower limit $R_{\min}$ increases rather slowly with decreasing energy and the upper limit $R_{\max}$ increases much more rapidly. At $E=4$ MeV, the bulk of the capture concentrates at the surface of the compound nucleus just beyond $\bar{R}=\langle R^2\rangle^{1/2}=3.85$ fm, while at low energies the very-low-density or tail region dominates, but nevertheless not to the exclusion of the surface region. By inspection, the 90% and 50% lower limits at zero energy are apparently near $N=16$ and 22, which are well within the surface region. Thus we are led to the conclusion that, in the capture reaction, the nuclear potential is sampled at all energies and should be properly considered even at astrophysical energies around 10 keV.[16]

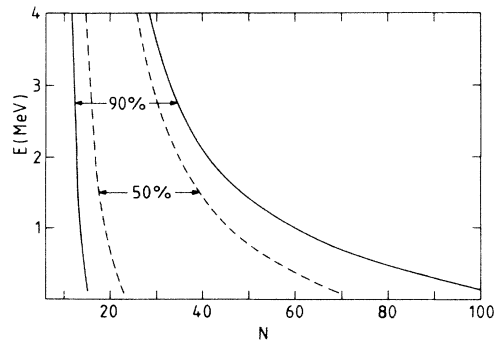

FIG. 2. Values of $R_{\min}$ and $R_{\max}$ for $P=0.5$ and 0.9 in the s-wave capture to the ^{7}Be ground state.

The procedure of Buck *et al.* attempts to construct just such a macroscopic potential. It is unavoidably an effective potential to simulate the many-body properties of the complete problem. An accurate construction must be able to reproduce all the important features which come from a microscopic quantal formulation. From RGM studies,[12] one learns that, because of antisymmetrization, the effective potential is nonlocal. For practical applications, many authors approximate the nonlocal character by constructing an equivalent local potential which is energy and parity dependent.

We discuss now the accuracy of the Gaussian potential of Eqs. (13) and (14) in this context. A local Gaussian potential, which reproduces $\langle R^2\rangle$ perfectly, will still lead to wave functions which exhibit the "Perey effect,"[17] i.e., in the range of the local potential the absolute magnitude of the local wave function is larger than their "nonlocal" counterpart. For bound states normalized to unity, this means that the magnitude of the asymptotic part of the local wave function is smaller than the nonlocal one. We see in Fig. 2 that at low energies it is the tail region which dominates. Therefore, this shortcoming of the local wave function at large separations may explain the difference between $S(0)=0.691$ keV b from A-RGM and $S(0)=0.515$ keV b from the Gaussian-potential model. However, this turns out to be not quite the case, because for the ground state, $N_{3/2}$ (A-RGM)=4.60 and $N_{3/2}$ (Gaussian)=4.40, where $N_{3/2}$ in these two cases are the asymptotic normalization constants with respect to the Whittaker function. The square of $N_{3/2}$ (A-RGM)/$N_{3/2}$ (Gaussian) gives an indication that, in this instance, the "Perey effect" amounts to approximately a 10% correction only to the Gaussian result. This does not account for the 34% difference between the A-RGM and the Gaussian S factors. This estimate of about 10% is confirmed in a calculation in which the capture matrix element is evaluated with an A-RGM bound state and a Gaussian-potential scattering state. Clearly, the rest of the discrepancy is due to the difference in the s waves.

It is possible to discuss together the energy dependence and the parity dependence of the effective local potential in our situation since our aim is to construct an s-wave potential for low-energy scattering which is different from the l-odd bound-state potential, although the energy-dependent effect itself may be quite small because the binding energies are only 1.58 and 1.15 MeV. The prescription according to Buck *et al.* to simulate these two effects is to readjust the central depth of the Gaussian potential to reproduce the s-wave scattering length. Such scaling prescription may be too crude to account for the parity dependence which has its origin in the three-nucleon or core exchange between ^{3}He and α.[18] There are indications of the qualitative difference between the l-even and l-odd effective potentials in the work of Furutani *et al.*[19] These authors used the following potentials:

$$V(R)=-103.4\exp(-0.2R^2)+13.8\exp(-0.091R^2)$$
$$(l=\text{even})\ , \tag{17}$$

$$V(R) = -86.2\exp(-0.2R^2)\ (l=\text{odd}) \tag{18}$$

between the t and α clusters in the framework of the orthogonality condition model (OCM) for the $2\alpha+t$ system to reproduce many experimental data. They pointed out that the difference between Eqs. (17) and (18) was crucial for their success. The similarity between the Gaussian potentials of Eqs. (13), (14), and (18) is noteworthy.

For our further investigation, we label two types of potentials for s-wave scattering between ^{3}He and α:

(i) Potential A:

$$V(R) = -\overline{V}\exp(-0.154R^2)\ , \tag{19}$$

where in potential $A1$, $\overline{V}=65.60$ MeV and in potential $A2$, $\overline{V}=69.81$ MeV.

(ii) Potential B:

$$V(R) = -\overline{V}\exp(-0.2R^2)+13.8\exp(-0.091R^2)\ , \tag{20}$$

where in potential $B1$, $\overline{V}=130.5$ MeV and in potential $B2$, $\overline{V}=120.79$ MeV.

In potential $A1$, $\overline{V}=65.60$ MeV reproduces the A-RGM scattering length of $a=28.2$ fm which we have encountered previously. In potential $A2$, $\overline{V}=69.81$ MeV reproduces the A-RGM phase shift (identical to the RGM phase shift) at $E=4.0$ MeV, displayed in Table I of LKT1. The parameters $\overline{V}$ in potentials $B1$ and $B2$ are from similar adjustments to reproduce, respectively, the A-RGM scattering length and the phase shift at $E=4.0$ MeV. Clearly, potential A is inspired by the prescription of Buck *et al.* and potential B by Eq. (17) from OCM. With the s waves from these potentials and extrapolating from cross sections at very low energies, we obtain

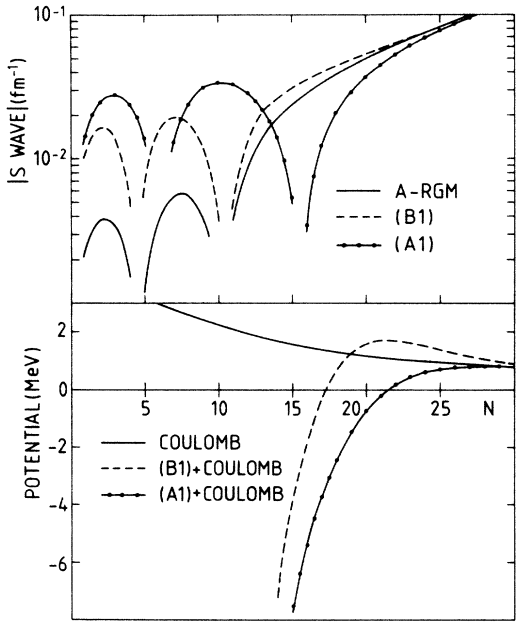

FIG. 4. In the upper part are shown the s-wave radial relative-motion functions from A-RGM and macroscopic models with potentials $A1$ and $B1$. In the lower part are shown the Coulomb potential, the [($A1$) + Coulomb] potential, and the [($B1$) + Coulomb] potential.

$S(0)=0.515$ keV b with potential $A1$,

$S(0)=0.569$ keV b with potential $A2$,

$S(0)=0.653$ keV b with potential $B1$,

$S(0)=0.604$ keV b with potential $B2$.

We find it useful to display them graphically in Fig. 3 and compare them with the RGM and A-RGM results. These S factors must still be corrected for the "Perey effect"

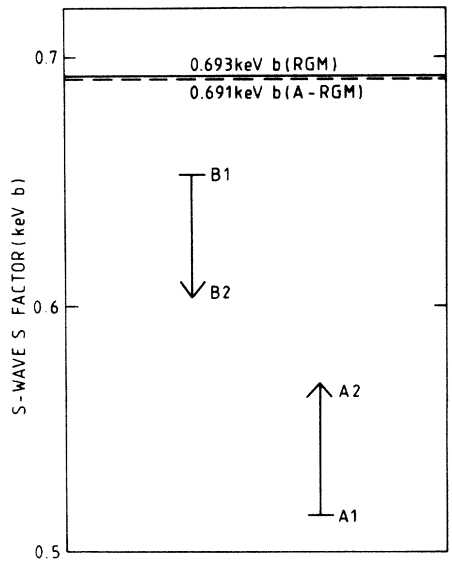

FIG. 3. The s-wave S factors of RGM, A-RGM, and macroscopic models with s-state potentials $A1$, $A2$, $B1$, and $B2$.

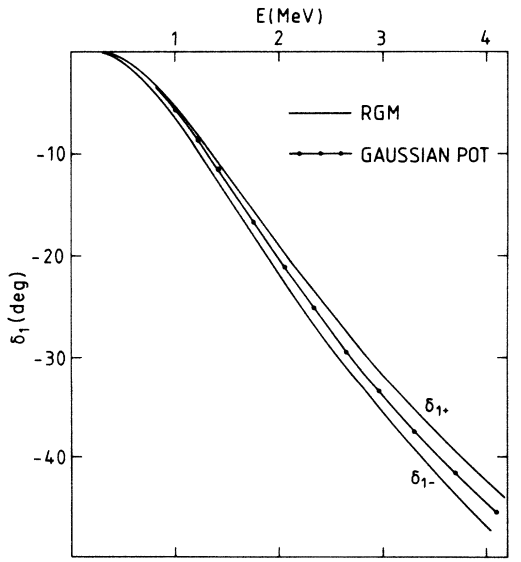

FIG. 5. Comparison of p-wave phase shifts from RGM and the Gaussian potential of Eq. (13).

which would increase their values by approximately 10%. Such correction notwithstanding, we have reason to believe that at this stage it is premature to pick a definite winner among the four potentials.

Using Fig. 2, we have argued that the surface region is of interest even at zero energy. We now plot potentials $A1$ and $B1$ as functions of N, as well as their s waves at $E=0.15$ MeV in Fig. 4 to examine this region closer. We have discussed earlier the non-negligible contribution to capture in the region of $N=15$–30. The s waves from potentials $A1$ and $B1$ are dramatically different in this range which is a direct reflection of the difference of the potentials. Below $N=15$, where the contribution to capture is insignificant, the difference in the wave functions is of no practical consequence. Above $N=30$, the s waves from the two potentials coincide with the A-RGM wave function—a clear indication that the nuclear potentials become negligible relative to the Coulomb potential. Since we are equipped with the A-RGM wave function in this case, we can say at a glance that potential $B1$ leads to a more accurate reproduction of the A-RGM results. However, in other capture-reaction cases where we do not have the RGM and A-RGM results, we would have no way to discriminate between potentials $A1$ and $B1$. The prescription of Buck *et al.* of using the scattering length is apparently not sufficient since, after all, both potentials give us the A-RGM scattering length. It seems that we require other nuclear information to constrain the construction of the macroscopic potential.

One class of information may be the phase shifts of the higher partial waves for a range of energies. We compare in Fig. 5 the odd p-wave phase shifts from A-RGM and the Gaussian potential of Eq. (13). The good agreement between them over an energy range of 4 MeV indicates that the potential is adequate for the l-odd states, which is also confirmed by the OCM calculation.[19] Perhaps it is not surprising that the Gaussian potential constructed from the electromagnetic properties of the l-odd bound states of ^{7}Be seems adequate for the l-odd phase shifts. In Figs. 6 and 7, we compare the even s- and d-wave phase shifts of A-RGM and potentials $A1$, $A2$, $B1$, and $B2$. Unfortunately, the A-RGM phase shifts do not distinctly favor one over the others. However, the fact that the results from these potentials are recognizably different from each other offers the insight that these even-l phase shifts are important data in the construction of a macroscopic potential for the l-even states.

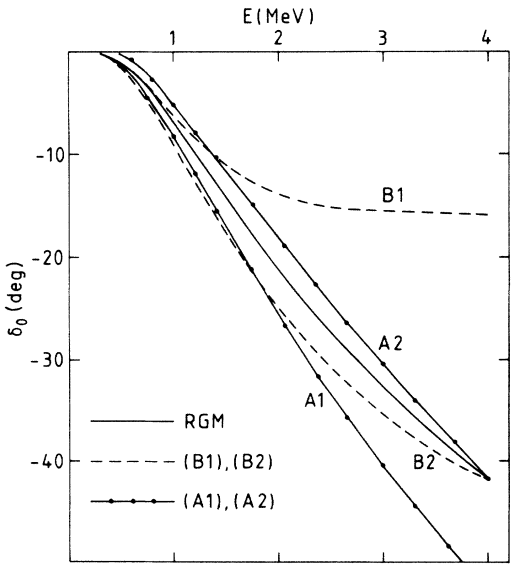

FIG. 6. Comparison of s-wave phase shifts from RGM and the potentials $A1$, $A2$, $B1$, and $B2$.

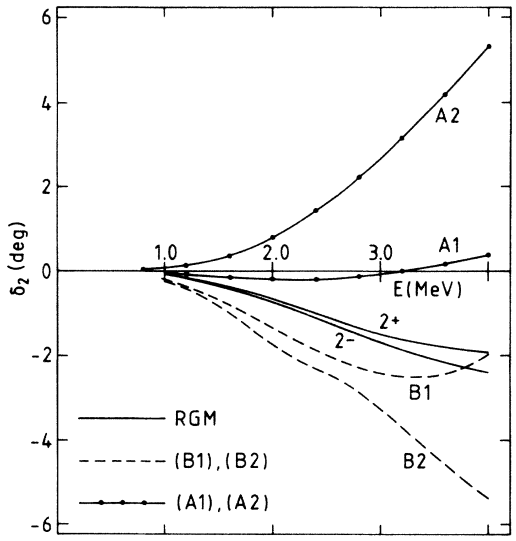

FIG. 7. Comparison of d-wave phase shifts from RGM and the potentials $A1$, $A2$, $B1$, and $B2$.

V. CONCLUSION

We have shown in this study that the A-RGM results for the electric-dipole radiative capture reaction ^{3}He$(\alpha,\gamma)^7$Be agree extremely well with RGM results over an energy range of 4 MeV, being almost perfect near zero energy and showing only a 2.7% discrepancy at 4 MeV. The A-RGM wave functions are derived directly from the microscopic RGM theory and they contain implicitly the important antisymmetrization property. Yet, its form and the details of the calculation can be compared directly with macroscopic models which try to simulate microscopic theories. From such comparisons we found evidence that the hard-core model[4,11] for the electric-dipole capture reaction near zero energy is not sufficiently accurate due to the neglect of the details of the nuclear interaction. Using the A-RGM results, we also showed that a recent suggestion on the construction of a macroscopic nuclear interaction[5] seems to be inadequate. Specifically, the odd-even difference in the potentials, which has its origin in antisymmetrization, is not sufficiently well represented. Obviously, an accurate macroscopic model is very desirable. To facilitate its construction, we suggest that other nuclear information, apart from those used in Ref. 5, may have to be taken into account.

This research was partially supported by the Supercomputer Institute at the University of Minnesota.

[1]Y. C. Tang, in *Clustering Aspects of Nuclear Structure,* edited by J. S. Lilley and M. A. Nagarajan (Reidel, Dordrecht, Holland, 1985).

[2]Q. K. K. Liu, H. Kanada, and Y. C. Tang, Z. Phys. A **303**, 253 (1981).

[3]H. Walliser and T. Fliessbach, Phys. Rev. C **31**, 2242 (1985).

[4]Z. R. Iwinski, L. Rosenberg, and L. Spruch, Phys. Rev. C **29**, 349 (1984).

[5]B. Buck, R. A. Baldock, and J. A. Rubio, J. Phys. G **11**, L1 (1985).

[6]D. N. Schramm and R. V. Wagoner, Annu. Rev. Nucl. Sci. **27**, 37 (1977).

[7]Q. K. K. Liu, H. Kanada, and Y. C. Tang, Phys. Rev. C **23**, 645 (1981).

[8]H. Horiuchi, Prog. Theor. Phys. (Suppl.) **62**, 90 (1977).

[9]J. A. Koepke, R. E. Brown, Y. C. Tang, and D. R. Thompson, Phys. Rev. C **9**, 823 (1974).

[10]H. Walliser, Q. K. K. Liu, H. Kanada, and Y. C. Tang, Phys. Rev. C **28**, 57 (1983).

[11]T. A. Tombrello and P. D. Parker, Phys. Rev. **131**, 2582 (1963).

[12]Y. C. Tang, M. LeMere, and D. R. Thompson, Phys. Rep. **47**, 167 (1978).

[13]Y. C. Tang, E. Schmid, and K. Wildermuth, Phys. Rev. **131**, 2631 (1963).

[14]H. Walliser, H. Kanada, and Y. C. Tang, Nucl. Phys. **A419**, 133 (1984).

[15]When we used the procedure of Buck *et al.* to calculate the S factors directly, we obtained $S(0)=0.527$ keV b and $S_{1/2}(0)/S_{3/2}(0)=0.453$. They differ only slightly from the results from extrapolation.

[16]Our present plot with A-RGM wave functions in Fig. 2 is more useful in a discussion of probability than a slightly different one in LKT1 where the RGM wave functions are used, since the relative-motion function in RGM, $f_{Jl}(R)$ in Eq. (1), is not directly amenable to a probability discussion because of the antisymmetrization operator.

[17]F. G. Perey, *Direct Interactions and Nuclear Interaction Mechanism,* edited by E. Clementel and C. Villi (Gordon and Breach, New York, 1963).

[18]Y. C. Tang, *Microscopic Description of the Nuclear Cluster Theory,* in Lecture Notes in Physics, Vol. 145 (Springer, Berlin, 1981).

[19]H. Furutani, H. Kanada, T. Kaneko, S. Nagata, H. Nishioka, S. Okabe, S. Saito, T. Sakuda, and M. Seya, Prog. Theor. Phys. (Suppl.) **68**, 193 (1980).